HHS Public Access

Author manuscript

Exp Neurol. Author manuscript; available in PMC 2023 November 27.

Published in final edited form as:

Exp Neurol. 2023 January ; 359: 114257. doi:10.1016/j.expneurol.2022.114257.

Annexin A1 upregulates hematoma resolution via the FPR2/p-ERK(1/2)/DUSP1/CD36 signaling pathway after germinal matrix hemorrhage

Jerry J. Flores[a], **Yan Ding**[a], **Prativa Sherchan**[a], **John H. Zhang**[a,b], **Jiping Tang**[a,*]

[a]Department of Physiology & Pharmacology, Loma Linda University School of Medicine, Loma Linda, CA, USA

[b]Departments of Anesthesiology and Neurosurgery, Loma Linda University School of Medicine, Loma Linda, CA, USA

Abstract

Germinal matrix hemorrhage (GMH) is one of the leading causes of morbidity and mortality in preterm infants in the United States, with little progress made in its clinical management. Blood clots disrupting normal cerebrospinal fluid circulation and absorption after germinal matrix hemorrhage are key contributors towards post-hemorrhagic hydrocephalus development. n-formyl peptide receptor 2 (FPR2), a G-protein-coupled receptor, has been associated with the activation of p-ERK1/2, which in turn promotes the transcription of the DUSP1 gene, which may play a role in CD36 signaling. CD36 scavenger, a transmembrane glycoprotein, plays an essential role in microglia phagocytic blood clot clearance after GMH. FPR2's role in blood clot clearance after hemorrhagic stroke is unknown. We hypothesize that FPR2 activation by FPR2 agonist Annexin A1 (AnxA1) will enhance hematoma resolution via the upregulation of the CD36 signaling pathway, thereby improving short- and long-term neurological outcomes. Bacterial collagenase (0.3 U) was infused intraparenchymally into the right hemispheric ganglionic eminence in P7 rat pups to induce GMH. AnxA1 and FPR2 Inhibitor (Boc2) were given at 1-h post-GMH via intranasal administration. FPR2 CRISPR was given 48-h prior to GMH induction. Short-term neurological deficits were assessed using negative geotaxis test. Hematoma volume was assessed using hemoglobin assay. Protein expression was assessed using western blots. Long-term neurocognitive deficits and motor coordination were assessed using Morris water maze, rotarod, and foot fault tests. We have demonstrated that AnxA1 treatment enhances hematoma resolution

*Corresponding author at: Department of Physiology and Pharmacology, Loma Linda University School of Medicine, Loma Linda, CA 92354, USA. Jtang@llu.edu (J. Tang).

Authors contributions

JF participated in the research design, methodology (including animal surgery, Western Blotting, and Immunohistochemistry), data analysis, and drafting/construction of the manuscript. YD and PS assisted with neurobehavior, data interpretation, and intracerebroventricular injection. JF, JHZ, and JT participated in research design and editing of the manuscript. JT, the corresponding author, participated in all aspects of the study, such as research design, data interpretation, and manuscript preparation. All authors have read and approved the final manuscript.

Declaration of Competing Interest

The authors of this manuscript declare that they have no known competing financial interests or personal relationships that could have appeared to influence the work reported in this paper.

Appendix A. Supplementary data

Supplementary data to this article can be found online at https://doi.org/10.1016/j.expneurol.2022.114257.

and improved short and long-term outcomes. Lastly, FPR2 agonist AnxA1 treatment resulted in the upregulation of the FPR2/p-ERK(1/2)/DUSP1/CD36 signaling pathway.

Keywords

AnxA1; FPR2; GMH; Hematoma resolution; Microglia; Microglia polarization; N-formyl peptide receptor 2; Annexin A1; M2; M1; Hemorrhagic stroke; Phagocytosis; Neonatal stroke, microglia activation

1. Introduction

Germinal matrix hemorrhage and intraventricular hemorrhage (GMH-IVH) is a leading cause of morbidity mortality in premature and or low birthweight infants, especially those born before 32 weeks of gestation (Strahle et al., 2012; Egesa et al., 2021). The site of hemorrhage occurs in the fragile capillary network of the subependymal germinal matrix of the neonatal brain, where ruptures of these fragile capillaries may be due to abrupt fluctuations in cerebral blood flow due to hemodynamic and cardiorespiratory instability (Ballabh, 2014). Debilitating consequences of GMH include the formation of post-hemorrhagic hydrocephalus (Ballabh, 2010; Heron et al., 2010). The expansion of the cerebroventricular system leads to mechanical compression and consequent injury of the surrounding brain tissue, causing neurological deficits in patients that survive the initial bleed. Intracerebroventricular blood clots have been identifed as causative factors of hydrocephalus formation. Blood clots directly impair the circulation and absorption of cerebrospinal fluid (CSF) (Whitelaw et al., 2004; Stein et al., 2010; Strahle et al., 2012; Li et al., 2018). FDA-approved therapeutics for stroke such as alteplase have been shown to cause hemorrhagic transformation and thus be an ineffective therapeutic for GMH (Yaghi, Willey et al., 2017). Additionally, current clinical management of hydrocephalus profoundly relies on the surgical insertion of shunts that drain excess CSF from the ventricles into the peritoneum, where it can be absorbed by the vasculature, yet this procedure can cause post-surgical complications, and shunts often become obstructed and must be replaced over time (Woernle et al., 2013). Therefore, a safe and non-invasive treatment for the reduction of blood clots early in the pathophysiology to reduce post-hemorrhagic hydrocephalus would be essential in the management of GMH.

The primary macrophages of the CNS are known as microglia, which have been shown to play a primary role in the innate immune response after injury. After hemorrhagic stroke, resident microglia and recruited macrophages can play either a harmful or protective role after CNS injury, which is dependent on the dominate microglia phenotype (London et al., 2013). M2 phenotype, also known as alternatively activated M2 microglia, are noted as being recruited to the site of the hematoma, where the blood clot is removed through the process of phagocytosis (Aronowski and Zhao, 2011; Flores et al., 2016). Quick microglia blood clot clearance after hemorrhagic stroke was shown to be benefcial after GMH (Flores et al., 2016). The quick removal of the blood clot after GMH serves as a benefcial target for this patient population.

N-formyl peptide receptor 2 (FPR2), a G-protein-coupled receptor, is expressed on microglia/macrophages in the central nervous system. FPR2 agonism has been shown to improve outcomes after stroke (McArthur et al., 2010; Bena et al., 2012; Ding et al., 2019). More specifcally, Annexin A1 (AnxA1) has been shown to stimulate FPR2 and promoted neuroprotection after hemorrhagic stroke, yt these neuroprotective effects were abolished with the administration of FPR2 antagonist N-tert-butyloxycarbonyl-Phe-Leu-Phe-Leu-Phe (Boc-2) (Ding et al., 2020). Additionally, FPR2 upregulation promoted monocyte recruitment and increased phagocytic activity (Ramon et al., 2014). FPR2 has been associated with the activation of phosphorylated extracellular-signal-regulated kinase 1/2 (p-ERK1/2), which in turn promotes the transcription of the dual-specifcity protein phosphatase 1 (DUSP1) gene (Finelli et al., 2013). Current literature suggests that DUSP1 may play a role in the upregulation of phagocytosis by macrophages, yet its importance in stroke has not been evaluated. Interestingly, FPR2 has been shown to upregulate scavenger receptor CD36, which plays a significant role in hematoma resolution (Cattaneo et al., 2013; Ramon et al., 2014). Additionally, FPR2 activation has also been found to polarize microglia into the M2 phenotype (Li et al., 2011), is primarily responsible for the mediation of wound healing and enhancement of macrophage phagocytosis of blood clots in GMH (Flores et al., 2016). Therefore, we hypothesized that FPR2 activation by FPR2 agonist AnxA1 would enhance hematoma resolution via the upregulation of the CD36 signaling pathway.

In this present study, we demonstrate that FPR2 agonism enhanced hematoma resolution, through the promotion of M2-like microglia which improved short- and long-term neurological deficits after GMH through the p-ERK(1/2)/DUSP1/CD36 signaling pathway.

2. Materials and methods

2.1. Animals

Animal usage, methods, and experimental design were approved by the Loma Linda University Institute Animal Care and Use Committee and in compliance with the ARRIVE Guidelines for the use of animals in research. 258 p7 Sprague-Dawley Neonatal pups (weight 9–15 g, Harlan, Livermore, CA) were used for this study.

2.2. Germinal matrix hemorrhage (GMH) model

Germinal Matrix Hemorrhage (GMH) was induced by stereo-guided injection of sterile bacterial collagenase as described in (Lekic et al., 2012). Neonatal rat pups were anesthetized with 5% isoflurane via isoflurane gas mixer, which were then adhered onto a stereotactic frame with a neonatal adaptor. An incision was made in the midline exposing the bregma, and a burr hole was made on the right side of the skill at coordinates of 1.6 mm (right-lateral), and 1.5 mm (rostral) from bregma. A 10 uL syringe with 0.3 units of collagenase V-II (VII-S, Sigma; 0.3U in 0.5μL of PBS) was guided through the burr hole at a depth of 2.7 mm, where the infusion of the collagenase occurred by a microinfusion pump ((Harvard Apparatus, Hollison, MA). To minimize the backflow of the collagenase, the syringe was kept in place for 5 min after the completion of infusion and was withdrawn at a rate of 0.5 mm/min. Pups were observed for changes in skin colour, temperature, respiratory rhythm and frequency, and heart rates. Once the needle was removed bone wax was used to

seal the burrhole, followed by the suturing of the incision line. Pups were then placed in a 37 °C heated blanket for recovery and then placed back with the dam. The sham group was only subjected to needle insertion without collagenase infusion.

2.3. CRISPR Intracerebroventricular injections

FPR2 CRISPR knockout (San Cruz Biotech, USA) plasmid or CRISPR control (Santa Cruz Biotech, USA) were given at a dose of 3 μg/pup. Animals were anesthetized with 5% isoflurane and a scalp incision was made on the skull surface where the bregma was exposed. A selected group of rats were given different reagents according to the project design and were injected with a 10-ul syringe (Hamilton, Nevada, USA) at the location of 1.3 mm posterior and 1.3 mm lateral to the bregma, and 1.7 mm deep to the skull surface at the contralateral hemisphere 48 h before GMH (2ul/rat pup). The control rat pup was injected with a CRISPR dilutant (Santa Cruz, Dallas, TX). The injection was completed in 5 min, and the needle was maintained in the injection position for an additional 2 min. The needle was removed slowly out of the brain, and the incision line was sutured. After recovery from anesthesia, the rat pups were placed back into their respective cages. Control CRISPR plasmid (Santa Cruz Biotech, Dallas, Tx) and FPR2 CRISPR were used. Sham animals received CRISPR Dilutant. The FPR2 CRISPR RNA sequence can be found in the supplemental material.

2.4. Drug administration, experimental design, and animal groups

FPR2 inhibitor N-tert-butyloxycarbonyl-Phe-Leu-Phe-Leu-Phe (Boc-2) (MP Biomedical, Irvine, CA) was intranasally administered 1-h after surgery or give for either 3 or 7 consecutive days depending on the time-point.

Both male and female P7 rat pups were randomly divided into the following groups: Sham-operated, GMH + Vehicle, GMH + AnxA1, GMH + AnxA1 + Boc-2, GMH + FPR2 CRISPR, GMH + FPR2 CRISPR, GMH + CRISPR Plasmid Control, GMH + CLOD, GMH + AnxA1 +CLOD. Fig. 1 shows each animal group and experimental design.

Experiment 1: Detecting the endogenous expression levels of FPR2 and DUSP1.—Western Blot (WB) was used to evaluate the expression of these proteins in whole-brain lysate at 12 h, 24 h, 72 h, 5d, and 7d after GMH. Additionally, to confirm if FPR2 and DUSP1 proteins were found on microglia cells, the colocalization of FPR2 or DUSP1 on microglia cells was done through immunohistochemistry. Nissl staining was also conducted at 72 h to indicate the structural location of IHC images.

Experiment 2: Evaluating the best dosing regimen and rout of administration of AnxA1.—Animals were divided randomly into two groups, which either received intraperitoneal or intranasal administration of Human recombinant Annexin A1 (AnxA1, R&D Systems) at a low and high concentration at 1 h after GMH induction and given for three consecutive days. Dosage concentrations for annexin A1 were modifed from the following study (Ding et al., 2020). The following groups were randomly assigned: Sham, GMH + Vehicle, GMH + AnxA1 (I·P, 0.5 μg/rat pup), GMH + AnxA1 (I·P 1.5 μg/rat pup), GMH + AnxA1(in 0.05 μg/ rat pup), and GMH + AnxA1 (0.0150 μg/rat pup). Hemoglobin

assay and short-term neurobehavior were used to evaluate the best dosing regimen at 72 h post-ictus.

Experiment 3: Evaluating the effects of FPR2 agonism via AnxA1 on short- and long-term after GMH.—FPR2 inhibitor Boc-2 (MP Biomedical, Irvine, CA) was given in combination with AnxA1 at 1 h post-ictus. Hemoglobin assay and short-term neurobehavior were conducted to evaluate the hematoma content and neurobehavioral deficits, respectively at 24 h, 72 h, and 72 h. Long-term behavior was conducted to assess long-term neurobehavioral deficits. Long-term animals were assessed for CSF pressure and Nissl staining was used to assess morphological changes (ventricular volume).

Experiment 4: Evaluating FPR2's role in microglia cells and its ability to polarize M1 microglia to M2 phenotype.—Immunohistochemistry was conducted at 72 h after GMH, where M1 marker (TNF-α) or M2 marker (Mannose Receptor) was colocalized with activated microglia (CD11b). Additionally, to determine the role of FPR2 in microglia induced hematoma resolution, Clophosome-A clodronate liposomes (FormuMax, Sunnyvale, CA) was used to decrease microglia cells populations in the CNS and given 48 h prior to GMH induction. Clophosome-A clodronate liposomes has been previously shown to selectively eliminate microglia (Kumamaru et al., 2012). To determine if the microglia cell population was successfully reduced, western blots and IHC were performed to measure the expression of Iba1 (microglia marker) in the CNS. At 72 h, hemoglobin assay was performed to determine if the hindrance of microglia cells would ameliorate FPR2 mediated hematoma removal.

Experiment 5: Investigating the mechanism of the proposed FPR2 signaling pathway.—Expression Levels of FPR2, p-ERK (1/2), DUSP1, and CD36 were detected by WB. At 72 h, hemoglobin assay was performed to determine if FPR2 CRISPR ameliorated the effects of AnxA1.

These methods are consistent with the recommendations of the Panel on Euthanasia of the American Veterinary Medical Association (AVMA) and have been approved by the Animal Care and Use Committee at Loma Linda University.

2.5. Western blot

Brain hemispheres were perfused with PBS, collected and snap frozen with liquid nitrogen and storage will occur at 80° Celsius. Cytosolic and nuclear fractionation extract were obtained from brain samples as described in (Lekic et al., 2012). Denatured protein extract (50 μg) was electrophoresed and transferred to a nitrocellulose membrane and probed with antibodies. The following proteins were detected by the primary antibodies for detecting Annexin A1 (1:1000, Cell Signaling), FPR2 (1:1000, Santa Cruz), DUSP1 (1:1000, Cell Signaling), Mannose Receptor (1:1000, Life Sciences), CD36 (1:1000, Santa Cruz), Iba-1 (1:1000, Abcam), and p-ERK1/2 (Thr202/Tyr204) respectively as described in previous study (Ma et al., 2011). The optical densities of the bands were visualized using ECL Plus or Li-Cor fluorescence technology and analyzed with Image J Software (NIH).

2.6. Immunohistochemistry

Immunohistochemistry was executed as previously described in (Flores et al., 2016). Pups were perfused under deep anesthesia with PBS followed by 4% formaldehyde. The brains were removed for post-fxation in formalin and dehydrated with 30% sucrose solution. Paraffn-embedded brains were then sectioned into 10-μm-thick slices via cryostat. Slices were stained with the following primary antibodies; FPR2 (1:1000, Santa Cruz), DUSP1 (1:1000, Cell Signaling), Mannose Receptor (1:1000, Life Sciences), CD36 (1:1000, Santa Cruz), Iba-1 (1:1000, Abcam), CD11b (1:1000, Abcam), TNF-α (1:2000, Abcam) at 4 °C overnight. Samples were then incubated with their respective fluorescence-conjugated secondary anti-bodies (1:200, Jackson ImmunoResearch Labs) for 2 h at room temperature, which were then dried and stained with Hardset mounting solution with Dapi (Fischer Scientific). The perihemorrhagic area was imaged using a DMi8 fluorescent microscope (Leica Microsystems, Buffalo Grove, IL) under a 200c Fold feld. To detect the proportion of Mannose Receptor and TNF-α positive activated microglia/macrophage cells, 4 felds surrounding the perihematomal region were used to count.

2.7. Neurobehavior examination

Short-term Neurobehavior: For up to 7 consecutive days after GMH both the righting reflex test and negative geotaxis were conducted to evaluate locomotor deficits. Long-term behavioral analysis: Long-term neurological outcomes were assessed with water maze, foot-fault and Rota rod tests at 4 weeks post GMH. The Rotarod assesses motor impairment, foot fault test assesses motor and proprioception function, and the Morris water maze test assesses learning, memory, and visual functions. All tests were conducted in a blinded manner.

Negative Geotaxis: Rat pups were oriented at a 45° downward angle, where the amount of time it takes the pup to recognize that it is on an incline and correct its positioning by making a 180-degree turn facing the top of the incline is recorded in 60-s durations. This exam was repeated three times for three consecutive days post-ictus. The Average of each day was taken for statistical analysis.

Morris Water Maze: Morris Water Maze was conducted at 4 weeks as described in (Lekic et al., 2012). In short, rats were released into a circular pool (110 diameters) filled with water. Spatial cues were placed on the pool walls where animals were then trained to find a submerged platform (11 cm diameter). Each animal went through 10 trials per day, where the time and distance it took the animals to find the platform was recorded. On the last day, Probe trial was conducted where the platform was removed, and the time spent in each quadrant was measured. An overhead camera in conjunction with Noldus Ethosvision (Noldus Ethovision; Noldus, Tacoma, WA tracking system) recorded the swim path and measured the swim distance, swim speeds, and time spent in probe quadrant.

Rotarod and Foot Fault: Rotarod and foot fault were conducted as described in (Flores et al., 2016). Rats were placed into the beams in the rotarod (7 cm diameter) and tested at starting speeds of 5 RPM or 10 RPM with acceleration at 2 RPM per 5 s. Falling latency

was recorded with the use of the Rotarod integrated photobeam (SD Instruments, San Diego, CA).

2.8. Hemoglobin assay

Spectrophotometric measurements were used to assess hemorrhagic volume as previously described in (Flores et al., 2016). Preserved forebrains were placed into individual glass tube where 3 mL of PBS is inserted. The forebrains were then homogenized for 60 s each (Tissue Misder Homogenizer; Fisher Scientific, Pittsburgh, PA) and processed through ultrasonication for 1 min to lyse erythrocyte membranes. The supernatant was then mixed with Drabkin's reagent (Sigma Aldrich, St Louis, Mn) and were left to react for 15 min. Absorbance was measured using a spectrophotometer (540 nm; Genesis 10uv; Thermo Fisher Scientific, Waltham, MA), and hemorrhagic volume (μL) was calculated based on a standard curve as routinely performed as described by (Lekic et al., 2012).

2.9. Intracranial pressure (ICP) measurements

At 4 weeks post-GMH, animals were anesthetized and mounted onto an adult stereotaxic frame. A midline incision was made to expose the atlanto-occipital membrane and the cisterna magna was punctured with a 26G Hamilton needle attached to a low-pressure transducer (Digi-Med LPA 400-low pressure Analyzer, Med-Louisville, Kentucky, USA) as described in (Lackner et al., 2013).

2.10. Ventricular volume

4-weeks after GMH, animals were anesthetized and euthanized, where the whole brains were extracted and prepared for histology similar to those prepared for IHC. Brains were embedded with optimal cutting temperature solution (OCT, Fisher Scientific, Waltham, MA) and sectioned into 24 μm thick slices. Samples were then stained with Cresyl violet solution (Fischer Scientific, Waltham, MA), where then optical dissector principles were used to delineate the cerebral structure borders as previously described in (Lekic et al., 2012). Morphometric analysis of samples involved hand delineation of the ventricular system which include the Lateral, third, cerebral aqueduct, and fourth ventricle. Ventricular volume was analyzed using ImageJ software (NIH). Volumes were calculated using the following equation: [(Average [(Area of coronal section) × Interval × Number of sections)] (MacLellan et al., 2008).

2.11. Rigor and statistical analysis

All animals used in this study were randomly numbered and sorted into each of the indicated animal groups using Excel. The following system was used to randomly assort the animals: 1) pups are sequenced vertically in Excel; 2) "RAND" function was used to generate a random number to each pup; 3) reranked the random numbers in an ascending or descending order; 4) lastly designate a certain number of pups into each animal group indicated in the experimental design. The assigned animal groups were unknown to researchers conducting the indicated methodology.

The number of animals needed per groups was determined using type 1 error at a rate of 0.05 and a power of 0.8 on a 2-sided test by power analysis. Data was represented as mean ±

SD. After normality is confirmed, parametric data will be analyzed using one-way ANOVA with Tukey's post-hoc test. *P* values <0.05 were considered as statistically significant. Graphpad Prism 7 was used for graphing and analyzing all data.

3. Results

3.1. The endogenous expression of FPR2 and AnxA1 increased after GMH

To determine how FPR2 and AnxA1 are affected by the GMH pathophysiology, a time-course study was conducted to examine these proteins by WB at 0 (Sham), 12-, 24-, and 72 h, and 5- and 7-days post-ictus. Endogenous expression of FPR2 was significantly increased at 72 h, where expression remained elevated at 7 days after GMH (Fig. 2 A and C). In Similar fashion, AnxA1 expression significantly elevated at 72 h after GMH and remained elevated for 7 Days (Fig. 2 A and Fig. 2 B). Both endogenous proteins demonstrated a similar trend in gradual increased expression after GMH. Based on these results, it can be suggested that endogenous AnxA1 may play a role in the upregulation of FPR2.

To determine if FPR2 receptor is present in the neonatal CNS, Double immunofluorescence staining was used for the cellular localization of both markers in microglia cells at 72 h after GMH. FPR2 expression was more prominent in microglia cells around the site of peri-hematoma 72 h after GMH (Fig. 3).

3.2. High-dose intranasal administration of human recombinant AnxA1 has the highest effcacy in decreasing hematoma content and improving short-term behavior

A dose-response study was conducted to determine the best dose and route of administration of AnxA1. AnxA1 was administered in low or high-dose and was given interpersonal (low, 0.5 μg/mg rat pup or High, 1.5 μg/mg rat pup) or intranasally (low, 0.05 μg or High, 0.150 μg per rat pup). Experimental design is described in experiment 2 (Fig. 1). Negative Geotaxis was conducted for 3 consecutive days and hemoglobin assay was examined at 72 h after GMH. At 24 h when compared to sham, all groups had significant neurological impairment (Fig. 4 A). At 48 h after GMH, all dosages and routes of administration showed a positive trend of improved neurobehavior at 48 and 74 h (Fig. 4A). Only the high dose intranasal AnxA1treatment significantly improved motor coordination when compared to vehicle at 48 and 72 h (Fig. 4 A). Furthermore, when compared to sham, high dose intranasal AnxA1 was not significantly different (Fig. 4 A). At 72 h when compared to the vehicle group, all dosing regiments and routes of administration were significantly effcient in reducing the hemoglobin content (Fig. 4 B). Additionally, High dose intranasal group was not significant to the sham group (Fig. 4 B). Based on these results we determined that the high dose of AnxA1 administered intranasally was the best dose and route of administration and will be used for the remainder of the experiments.

3.3. Intranasal administration of human recombinant AnxA1 improves short- and long-term outcomes after GMH

To determine if the neuroprotective effects of AnxA1 are through the activation of FPR2, FPR antagonist Boc-2 was given in combination with treatment. Animals were randomly divided into 4 groups as described in experiment 3 (Fig. 1). At 48- and 72 h, Boc-2

significantly reversed the protective effects of AnxA1 on motor coordination (Fig. 5). Additionally, pharmacological inhibition of FPR2 significantly attenuated AnxA1's effects on the reduction of hematoma content at 72 h and 7 days after GMH (Fig. 6). No significance was seen at 24 h post-GMH among treatment and inhibitor (Fig. 6). Thus, this data demonstrates that AnxA1 effects on hematoma resolution were mediated through FPR2 agonism in the short-term.

We further assessed the effects of AnxA1 on long-term outcomes (long-term neurological function (spatial memory, reference memory, and motor coordination). Animals were assigned randomly to each group described in Experiment 3 (Fig. 1). Neurological function was performed at 4 weeks after GMH for 5 consecutive days. During the Probe Trial of the Morris water maze, the vehicle group spent significantly less time in the platform quadrant when compared to the sham group, whereas AnxA1 treated animals spent more time in the platform quadrant when compared to Vehicle group (Fig. 7 C and D). AnxA1 treatment also significantly improved sensorimotor function in the foot fault test (Fig. 7 A) and motor coordination in the Rotarod test (Fig. 7 B) when compared to Vehicle group. Yet, these improvements in reference memory, sensorimotor, motor coordination were reversed by FPR2 antagonist Boc-2 (Fig. 7).

At the end of long-term neurobehavior test, animals were evaluated for intracranial pressure (ICP), as it is an indicator of the formation of hydrocephalus. At the end points of the long-term study, brain tissues were extracted and processed for histology to examine morphological changes in all animal groups. ICP was significantly decreased in the AnxA1 treated group when compared to vehicle and FPR2 antagonist groups (Fig. 8 C). For changes in brain morphology, ventricular volume was assessed at 4 weeks post-ictus. Additionally, ventricular volume was significantly increased in vehicle and FPR2 antagonist groups, yet AnxA1 treatment reduced post-hemorrhagic ventricular dilation (Fig. 8 A and B).

3.4. AnxA1 treatment enhanced M2 microglia/macrophage cells 72 h after GMH

Mannose Receptor (M2 marker) or TNF-Alpha was colocalized with CD11b to determine the amount of M1 or M2 microglia/macrophage cells at the site of perihematomal and were quantifed as described in (Flores et al., 2016). At 72 h after GMH, Mannose receptor positive microglia/macrophage cells were significantly increased in treated animals when compared among all groups (Fig. 9 A and B). Furthermore, AnxA1 treatment significantly decreased TNF-α positive microglia/ macrophage cells when compared to the vehicle and FPR2 inhibitor group (Fig. 10 A and B). This data demonstrates that AnxA1 treatment significantly increased M2 populations and decreased M1 microglia populations.

To determine if the actions of FPR2 agonism were mediated through microglia cells, animals were given i.c.v. injection of clodronate liposomes 2 days prior to GMH induction. WB was used at 24 h to examine the expression levels Iba1 in clodronate liposomes animals and hemoglobin assay was conducted at 72 h after GMH. At 24 h after GMH, Iba1 expression was significantly decreased when compared to the sham (Fig. 11 A). At 24 h, immunohistochemistry demonstrated that expression was less readily expressed on microglia cells in GMH animals that received clodronate liposomes (Fig. 11 B). At 72 h after GMH, hemoglobin assay established that AnxA1 treatment was unsuccessful in

reducing the blood clot when compared to sham, and there was no significant difference when compared to the Vehicle control (Fig. 11 C). Although clodronate liposomes did not eliminate completely eliminate microglia cell populations, these results suggests that FPR2 agonism mediates its hematoma resolution actions through microglia cells.

3.5. FPR2 stimulation activated p-ERK(1/2)/DUSP1/CD36 signaling pathway

FPR2 has been shown to activate p-ERK(1/2), which plays a role in the activation of DUSP1 (Ramon et al., 2014) (Finelli et al., 2013). FPR2 and DUSP1 have been shown to play a role in phagocytosis and activation of scavenger receptor CD36 (Cattaneo et al., 2013; Ramon et al., 2014). Thus, we evaluated the effects of AnxA1 on FPR2, ERK (1/2), DUPS1, and CD36 protein expression at 72 h after GMH. AnxA1 treatment significantly increased the expression of FPR2, p-ERK (1/2), DUSP1, and CD36 when compared to the sham and the Vehicle Group (Fig. 12 A, B, C, D, E respectively). Whereas FPR2 inhibitor attenuated the up regulation of these proteins (Fig. 12).

To further investigate the signaling pathway mechanism, CRISPR targeting FPR2 was used to determine if the signaling pathway would be affected after AnxA1 treatment. Animals were randomly assigned as detailed in the experimental design of Experiment 5. FPR2 CRISPR significantly decreased the expression of FPR2, p-ERK (1/2), DUSP1, and CD36 when compared to the control group that received AnxA1 72 h after GMH (Fig. 13). Additionally, WB was conducted to determine if FPR2 CRISPR would inhibit the neuroprotective effects of AnxA1 on FPR2 agonism at 72 h post-GMH. At 72 h after GMH, FPR2 CRISPR significantly inhibited the AnxA1 induced hematoma resolution (Fig. 13 F).

4. Discussion

GMH is one of the leading causes of mortality and morbidity in premature infants; debilitating consequences of GMH include the formation of post-hemorrhagic hydrocephalus, cerebral palsy, and motor and cognitive deficits (Ballabh, 2010; Heron et al., 2010; Koschnitzky et al., 2018). Intracerebroventricular blood clots have been identified as causative factors of hydrocephalus formation, as the blood clots directly impairs the circulation and absorption of cerebrospinal fluid (CSF) (Whitelaw et al., 2004; Stein et al., 2010; Li et al., 2018). The enhancement of hematoma resolution neuroprotective in adult and neonatal hemorrhagic stroke (Zhao et al., 2015; Flores et al., 2016; Liu et al., 2021). Our research group previously demonstrated that stimulation of signaling pathways that upregulate scavenger receptors CD36 and CD163 in microglia/macrophages lead to the rapid hematoma resolution after Germinal Matrix Hemorrhage (Flores et al., 2016, Liu et al., 2021). In this study, we examined the effects of FPR2 stimulation, via AnxA1, on hematoma resolution as well as its effects on short- and long-term outcomes after germinal matrix hemorrhage. Additionally, we determined if FPR2 inhibition reversed the observed beneficial effects of FPR2 agonism. This is the first study to investigate a completely new mechanism of action for FPR2 in hemorrhagic stroke for the enhancement of hematoma resolution and first to evaluate the therapeutic potential for attenuating post-hemorrhagic hydrocephalus and neurological deficits in the short- and long-term.

N-formyl peptide receptors (FPR) belong to a family of G-protein-coupled receptors expressed on microglia in the central nervous system. Stimulation of the n-formyl peptide receptor 2 (FPR2) by Annexin A1 (AnxA1) has been shown to be neuroprotective in models of stroke (McArthur et al., 2010; Bena et al., 2012). Although FPR2 has been previously studied in adult stroke, it is unclear if FPR2 is readily expressed in the neonatal CNS. Our time-course results suggest that after GMH, FPR2 expression steadily increased after GMH and reached significance from sham at 72 h and remained elevated for up to 7 days, indicating that FPR2 may play a role after GMH (Fig. 2 C). Immunohistochemistry confirmed that FPR2 was detected on microglia cells, indicating that FPR2 may play a beneficial role in the modulation of microglia cells (Fig. 3).

AnxA1 is a Ca2 + −dependent phospholipid-binding protein and an endogenous activator of FPR2 (Gavins et al., 2007). Our research group has previously demonstrated that FPR2 stimulation via AnxA1 improved neurological outcomes after adult hemorrhagic stroke (Ding et al., 2020). The role of FPR2 agonism via AnxA1 in hematoma resolution remains unknown in neonatal stroke. A time-course was conducted to determine if endogenous AnxA1 and FPR2 shared similar expression levels after stroke, we demonstrated that both proteins reached significance at 72 h after GMH (Fig. 2 B). These results indicated that both proteins play an active role in the GMH pathophysiology, thus we conducted a dose-response study to assess the best therapeutic dose and route of recombinant Annexin A1 administration, with specific interest in hematoma resolution, neurobehavioral outcomes, and post-hemorrhagic hydrocephalus. Our dose-response study demonstrated that the high dose of AnxA1 (0.150 μg/per rat pup) administered intranasally was most beneficial in increasing hematoma resolution (Fig. 3) and attenuating neurobehavioral deficits (Fig. 3) at 72 h after GMH induction. Pharmacological inhibition of FPR2 was adapted from our previous study (Ding et al., 2020), where FPR2 antagonist Boc2 ameliorated the beneficial effects of AnxA1 on hematoma resolution (Fig. 6) and improvements in neurobehavioral function at 72 h (Fig. 5). Furthermore, in our long-term study we found that therapeutic regiments of intranasal AnxA1 resulted in improved cognitive and motor function at 4 weeks after GMH induction (Fig. 7). In agreement with the long-term results, AnxA1 significantly reduced intracranial pressure (Fig. 8 C) and reduced ventricular dilation (Fig. 8 A and B) brought on by GMH at 4 weeks post-ictus. In contrast, Boc2 inhibition of FPR2 reversed the therapeutic effects of AnxA1 treatment in all long-term outcomes.

FPR2 activation has also been found to polarize microglia into the M2 phenotype (Li et al., 2011), primarily responsible for mediating wound healing and enhancing macrophage phagocytosis of blood clots in GMH (Flores et al., 2016). These findings suggest that FPR2 may play a significant role in immunomodulation that provides protection against multiple maladies. M2 phenotype has been shown to be vital in the repair mechanisms after stroke and plays a key role in removing neurotoxic iron from the injury inflicted area, providing further neuroprotection (Flores et al., 2016; Klebe et al., 2017). Yet M2's role in germinal matrix hemorrhage has been greatly understudied, further characterization of microglia subtypes and function needs to be conducted in the neonatal CNS. Our research group was the first to demonstrate that M2 polarization after GMH resulted in the enhancement of hematoma blood clot clearance and demonstrated that the activation of various signaling pathways that stimulated this microglia state had beneficial effects after

GMH (Flores et al., 2016; Liu et al., 2021). FPR2 stimulated, via AnxA1, significantly increased the number of M2 positive microglia cells at the site of peri-hematoma (Fig. 9). Additionally, AnxA1 treatments significantly reduced the population of M1 positive microglia cells at the site of peri-hematoma (Fig. 10). The introduction of FPR2 inhibitor Boc2 reversed the polarization of microglia cells. To establish that FPR2 therapeutic effects were executed through the stimulation of microglia cells, animals were given i.c.v. injections of clodronate liposomes to globally inhibit microglia cells in the CNS. Western blot demonstrated a decreased expression of microglia marker Iba1 at 24 h after GMH (Fig. 11A). Furthermore, immunohistochemistry conducted at 24 h after GMH indicated the inhibition of microglia cells in the CNS as there was low expression of microglia cells after GMH (Fig. 11 B). Lastly, Hemoglobin assay at 72 h demonstrated that the inhibition of microglia cells resulted in the attenuation of AnxA1's therapeutic effect on the hematoma blood clot, where no significance was found in hematoma content between the Vehicle control, Vehicle+clodronate liposomes, and clodronate liposomes+AnxA1 groups (Fig. 11 C), yet all groups were significant to the Vehicle+AnxA1 group. The data indicates the link between hematoma resolution, microglia, and FPR2 agonism.

FPR2 signaling has been associated with the activation of ERK1/2, which in turn promotes the transcription of the DUSP1 gene (Arthur and Ley, 2013; Finelli et al., 2013). Current literature suggests that DUSP1 may play a role in CD36 signaling (Wancket et al., 2012). Interestingly, FPR2 stimulation has been shown to mediate CD36 scavenger and has also been reported to transform microglia into phagocytes (Cattaneo et al., 2013; Ramon et al., 2014). CD36 play an important role in mediating phagocytosis and transfection of CD36 on cells lacking phagocytic abilities acquired this function (Ren et al., 1995). Thus, it is deducible that p-ERK/DUSP1/CD36 pathway is a potential mechanism by which FPR2 stimulation increases hematoma absorption. In this study we examined the underlying phagocytic mechanism of FPR2. We first co-treated the neonatal pups with FPR2 pharmacological antagonist Boc-2 and agonist AnxA1to determine if AnxA1 treatment elicits its neuroprotective effects through the agonism of the proposed FPR2 signaling pathway. At 72 h, WB data showed that AnxA1 treatment significantly increased the expression of FPR2, p-ERK(1/2), DUSP1, and CD36 when compared to all other groups (Fig. 12 A–E). Whereas introduction of Boc-2 significantly reduced the expression of all proteins. This suggests that AnxA1 neuroprotective effects are modulated through FPR2 stimulation and all signaling proteins. To further confirm these results, FPR2 CRISPR was administered to neonatal pups 48 h prior to GMH modeling. Western blot results showed that the introduction of FPR2 CRISPR significantly reduced the expression of the protein levels of FPR2, p-ERK(1/2), DUSP1, and CD36 when compared to the CRISPR control group that received AnxA1 treatment (Fig. 13 A–E). Lastly, to determine if the knock-down of FPR2 via CRISPR inhibited the effects of FPR2 on hematoma resolution, hemoglobin assay was conducted at 72 h. FPR2 CRISPR significantly ameliorated the resolution of hematoma (Fig. 13F). This data illustrates that the neuroprotective effects of FPR2 agonism are mediated through the FPR2/p-ERK(1/2)/DUSP1/CD36 signaling pathway.

Although our short and long-term data demonstrated the actions and signaling pathway of FPR2 agonism, there are limitations to this study. First, this study does not investigate the microglia subtypes involved in FPR2 agonism. More specifically, M2 microglia are

divided into three subtypes- M2a, M2b, M2c. Where both M2b and M2c participate in phagocytosis and removal of tissue debris, while M2a plays a role in cell regeneration (Roszer, 2015). Further characterization of M2 subtypes and function needs to be conducted. Second, this study briefly investigates the role of FPR2 in the formation of post-hemorrhagic hydrocephalus formation. Although intracranial pressures and ventricular volume were measured, FPR2 role in iron overload and CSF production was not, which are very important parameters of PHH (Li et al., 2018). Third, only microglia cells were investigated in this study. FPR2 is located on various other monocytes as well as astrocytes. Further experiments must be conducted so that the function of FPR2 on other cell types can be established in GMH. Fourth, AnxA1-FPR2 might trigger multiple intracellular signaling pathways and the signaling network can complicate this study. Interestingly, C/EBP alpha transcription factor is also upregulated by p-ERK1/2 and has been known to activate CD36 transcription in the nucleus which induces CD36 receptor activation (Muto et al., 2013). Recently, C/EBP alpha has shown to be upregulated in the CNS, more specifically in rat primary cultured microglia cells (Ramberg et al., 2011). Fifth, sham animals did not receive injections of PBS vehicle, this is a flaw in the experimental design as it may potentially cause intraparenchymal volume pressure which could produce a micro-hemorrhage. In future studies, there will be a consideration for the use of injections of PBS vehicle in sham animals.

Supplementary Material

Refer to Web version on PubMed Central for supplementary material.

Funding and fnancial disclosures

This study was support in part by National Institutes of Health grant 5R01NS117364-02 and the American Heart Association 20PRE35211027.

Data availability

Data will be made available on request.

Availability of data and materials

All data and information used in this current study are available from the corresponding author on reasonable request.

References

Aronowski J, Zhao X, 2011. Molecular pathophysiology of cerebral hemorrhage: secondary brain injury. Stroke 42 (6), 1781–1786. [PubMed: 21527759]

Arthur JS, Ley SC, 2013. Mitogen-activated protein kinases in innate immunity. Nat. Rev. Immunol 13 (9), 679–692. [PubMed: 23954936]

Ballabh P, 2010. Intraventricular hemorrhage in premature infants: mechanism of disease. Pediatr. Res 67 (1), 1–8. [PubMed: 19816235]

Ballabh P, 2014. Pathogenesis and prevention of intraventricular hemorrhage. Clin. Perinatol 41 (1), 47–67. [PubMed: 24524446]

Bena S, Brancaleone V, Wang JM, Perretti M, Flower RJ, 2012. Annexin A1 interaction with the FPR2/ALX receptor: identifcation of distinct domains and downstream associated signaling. J. Biol. Chem 287 (29), 24690–24697. [PubMed: 22610094]

Cattaneo F, Parisi M, Ammendola R, 2013. Distinct signaling cascades elicited by different formyl peptide receptor 2 (FPR2) agonists. Int. J. Mol. Sci 14 (4), 7193–7230. [PubMed: 23549262]

Ding Y, Flores J, Klebe D, Li P, McBride DW, Tang J, Zhang JH, 2019. Annexin A1 attenuates neuroinflammation through FPR2/p38/COX-2 pathway after intracerebral hemorrhage in male mice. J. Neurosci. Res 98 (1), 168–178. [PubMed: 31157469]

Ding Y, Flores J, Klebe D, Li P, McBride DW, Tang J, Zhang JH, 2020. Annexin A1 attenuates neuroinflammation through FPR2/p38/COX-2 pathway after intracerebral hemorrhage in male mice. J. Neurosci. Res 98 (1), 168–178. [PubMed: 31157469]

Egesa WI, Odoch S, Odong RJ, Nakalema G, Asiimwe D, Ekuk E, Twesigemukama S, Turyasiima M, Lokengama RK, Waibi WM, Abdirashid S, Kajoba D, Kumbakulu PK, 2021. Germinal matrix-intraventricular hemorrhage: a tale of preterm infants. Int. J. Pediatr 2021, 6622598. [PubMed: 33815512]

Finelli MJ, Murphy KJ, Chen L, Zou H, 2013. Differential phosphorylation of Smad1 integrates BMP and neurotrophin pathways through Erk/Dusp in axon development. Cell Rep 3 (5), 1592–1606. [PubMed: 23665221]

Flores JJ, Klebe D, Rolland WB, Lekic T, Krafft PR, Zhang JH, 2016. PPARgamma-induced upregulation of CD36 enhances hematoma resolution and attenuates long-term neurological deficits after germinal matrix hemorrhage in neonatal rats. Neurobiol. Dis 87, 124–133. [PubMed: 26739391]

Gavins FN, Dalli J, Flower RJ, Granger DN, Perretti M, 2007. Activation of the annexin 1 counter-regulatory circuit affords protection in the mouse brain microcirculation. FASEB J. 21 (8), 1751–1758. [PubMed: 17317721]

Heron M, Sutton PD, Xu J, Ventura SJ, Strobino DM, Guyer B, 2010. Annual summary of vital statistics: 2007. Pediatrics 125 (1), 4–15. [PubMed: 20026491]

Klebe D, Flores JJ, McBride DW, Krafft PR, Rolland WB, Lekic T, Zhang JH, 2017. Dabigatran ameliorates post-haemorrhagic hydrocephalus development after germinal matrix haemorrhage in neonatal rat pups. J. Cereb. Blood Flow Metab 37 (9), 3135–3149. [PubMed: 28155585]

Koschnitzky JE, Keep RF, Limbrick DD Jr., McAllister JP 2nd, Morris JA, Strahle J, Yung YC, 2018. Opportunities in posthemorrhagic hydrocephalus research: outcomes of the hydrocephalus association Posthemorrhagic hydrocephalus workshop. Fluids Barriers CNS 15 (1), 11. [PubMed: 29587767]

Kumamaru H, Saiwai H, Kobayakawa K, Kubota K, van Rooijen N, Inoue K, Iwamoto Y, Okada S, 2012. Liposomal clodronate selectively eliminates microglia from primary astrocyte cultures. J. Neuroinflammation 9, 116. [PubMed: 22651847]

Lackner P, Vahmjanin A, Hu Q, Krafft PR, Rolland W, Zhang JH, 2013. Chronic hydrocephalus after experimental subarachnoid hemorrhage. PLoS One 8 (7), e69571. [PubMed: 23936048]

Lekic T, Manaenko A, Rolland W, Krafft PR, Peters R, Hartman RE, Altay O, Tang J, Zhang JH, 2012. Rodent neonatal germinal matrix hemorrhage mimics the human brain injury, neurological consequences, and post-hemorrhagic hydrocephalus. Exp. Neurol 236 (1), 69–78. [PubMed: 22524990]

Li Y, Cai L, Wang H, Wu P, Gu W, Chen Y, Hao H, Tang K, Yi P, Liu M, Miao S, Ye D, 2011. Pleiotropic regulation of macrophage polarization and tumorigenesis by formyl peptide receptor-2. Oncogene 30 (36), 3887–3899. [PubMed: 21499310]

Li Q, Ding Y, Krafft P, Wan W, Yan F, Wu G, Zhang Y, Zhan Q, Zhang JH, 2018. Targeting germinal matrix hemorrhage-induced overexpression of sodium-coupled bicarbonate exchanger reduces Posthemorrhagic hydrocephalus formation in neonatal rats. J. Am. Heart Assoc 7 (3).

Liu S, Flores JJ, Li B, Deng S, Zuo G, Peng J, Tang J, Zhang JH, 2021. IL-20R activation via rIL-19 enhances hematoma resolution through the IL-20R1/ERK/Nrf2 pathway in an experimental GMH rat pup model. Oxidative Med. Cell. Longev 2021, 5913424.

London A, Cohen M, Schwartz M, 2013. Microglia and monocyte-derived macrophages: functionally distinct populations that act in concert in CNS plasticity and repair. Front. Cell. Neurosci 7, 34. [PubMed: 23596391]

Ma Q, Huang B, Khatibi N, Rolland W 2nd, Suzuki H, Zhang JH, Tang J, 2011. PDGFR-alpha inhibition preserves blood-brain barrier after intracerebral hemorrhage. Ann. Neurol 70 (6), 920–931. [PubMed: 22190365]

MacLellan CL, Silasi G, Poon CC, Edmundson CL, Buist R, Peeling J, Colbourne F, 2008. Intracerebral hemorrhage models in rat: comparing collagenase to blood infusion. J. Cereb. Blood Flow Metab 28 (3), 516–525. [PubMed: 17726491]

McArthur S, Cristante E, Paterno M, Christian H, Roncaroli F, Gillies GE, Solito E, 2010. Annexin A1: a central player in the anti-inflammatory and neuroprotective role of microglia. J. Immunol 185 (10), 6317–6328. [PubMed: 20962261]

Muto C, Yachi R, Aoki Y, Koike T, Igarashi O, Kiyose C, 2013. Gamma-tocotrienol reduces the triacylglycerol level in rat primary hepatocytes through regulation of fatty acid metabolism. J. Clin. Biochem. Nutr 52 (1), 32–37. [PubMed: 23341695]

Ramberg V, Tracy LM, Samuelsson M, Nilsson LN, Iverfeldt K, 2011. The CCAAT/ enhancer binding protein (C/EBP) delta is differently regulated by fbrillar and oligomeric forms of the Alzheimer amyloid-beta peptide. J. Neuroinflammation 8, 34. [PubMed: 21492414]

Ramon S, Bancos S, Serhan CN, Phipps RP, 2014. Lipoxin a(4) modulates adaptive immunity by decreasing memory B-cell responses via an ALX/FPR2-dependent mechanism. Eur. J. Immunol 44 (2), 357–369. [PubMed: 24166736]

Ren Y, Silverstein RL, Allen J, Savill J, 1995. CD36 gene transfer confers capacity for phagocytosis of cells undergoing apoptosis. J. Exp. Med 181 (5), 1857–1862. [PubMed: 7536797]

Roszer T, 2015. Understanding the mysterious M2 macrophage through activation markers and effector mechanisms. Mediat. Inflamm 2015, 816460.

Stein M, Luecke M, Preuss M, Boeker DK, Joedicke A, Oertel MF, 2010. Spontaneous intracerebral hemorrhage with ventricular extension and the grading of obstructive hydrocephalus: the prediction of outcome of a special life-threatening entity. Neurosurgery 67 (5), 1243–1251 (discussion 1252). [PubMed: 20948399]

Strahle J, Garton HJ, Maher CO, Muraszko KM, Keep RF, Xi G, 2012. Mechanisms of hydrocephalus after neonatal and adult intraventricular hemorrhage. Transl. Stroke Res 3 (Suppl. 1), 25–38. [PubMed: 23976902]

Wancket LM, Meng X, Rogers LK, Liu Y, 2012. Mitogen-activated protein kinase phosphatase (Mkp)-1 protects mice against acetaminophen-induced hepatic injury. Toxicol. Pathol 40 (8), 1095–1105. [PubMed: 22623522]

Whitelaw A, Cherian S, Thoresen M, Pople I, 2004. Posthaemorrhagic ventricular dilatation: new mechanisms and new treatment. Acta Paediatr. Suppl 93 (444), 11–14. [PubMed: 15035455]

Woernle CM, Winkler KM, Burkhardt JK, Haile SR, Bellut D, Neidert MC, Bozinov O, Krayenbuhl N, Bernays RL, 2013. Hydrocephalus in 389 patients with aneurysm-associated subarachnoid hemorrhage. J. Clin. Neurosci 20 (6), 824–826. [PubMed: 23562295]

Yaghi S, Willey JZ, Cucchiara B, Goldstein JN, Gonzales NR, Khatri P, Kim LJ, Mayer SA, Sheth KN, Schwamm LH, C. American Heart Association Stroke, C. Council on, N. Stroke, C. Council on Clinical, C. Council on Quality of and R. Outcomes, 2017. Treatment and outcome of hemorrhagic transformation after intravenous Alteplase in acute ischemic stroke: a Scientific statement for healthcare professionals from the American Heart Association/American Stroke Association. Stroke 48 (12), e343–e361. [PubMed: 29097489]

Zhao XR, Gonzales N, Aronowski J, 2015. Pleiotropic role of PPARgamma in intracerebral hemorrhage: an intricate system involving Nrf2, RXR, and NF-kappaB. CNS Neurosci. Ther 21 (4), 357–366. [PubMed: 25430543]

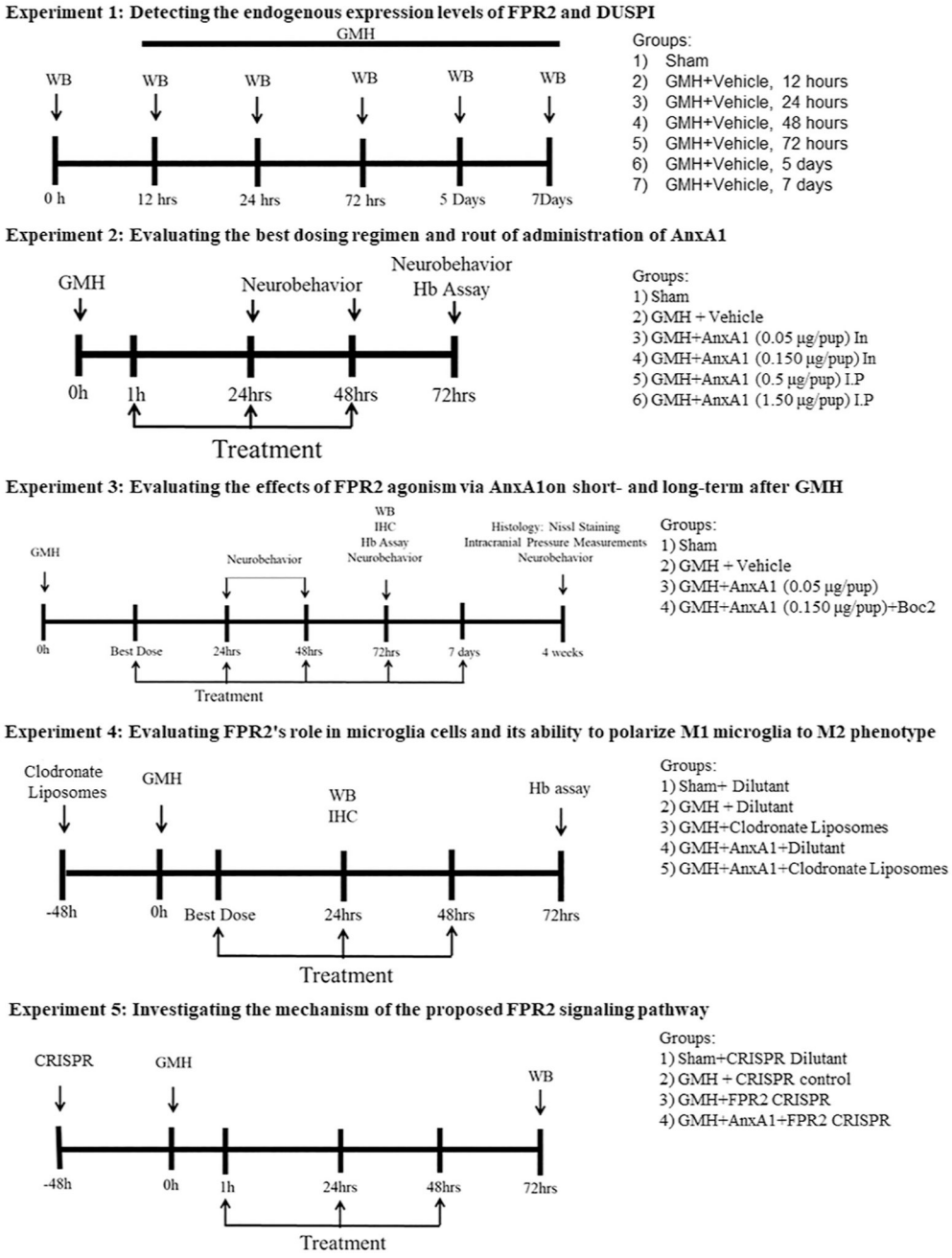

Fig. 1.

Experimental Design and Animal Groups. (GMH: Germinal Matrix Hemorrhage, WB: Western Blot, Hb Assay: Hemoglobin Assay, AnxA1: Annexin A1, IHC: Immunohistochemistry).

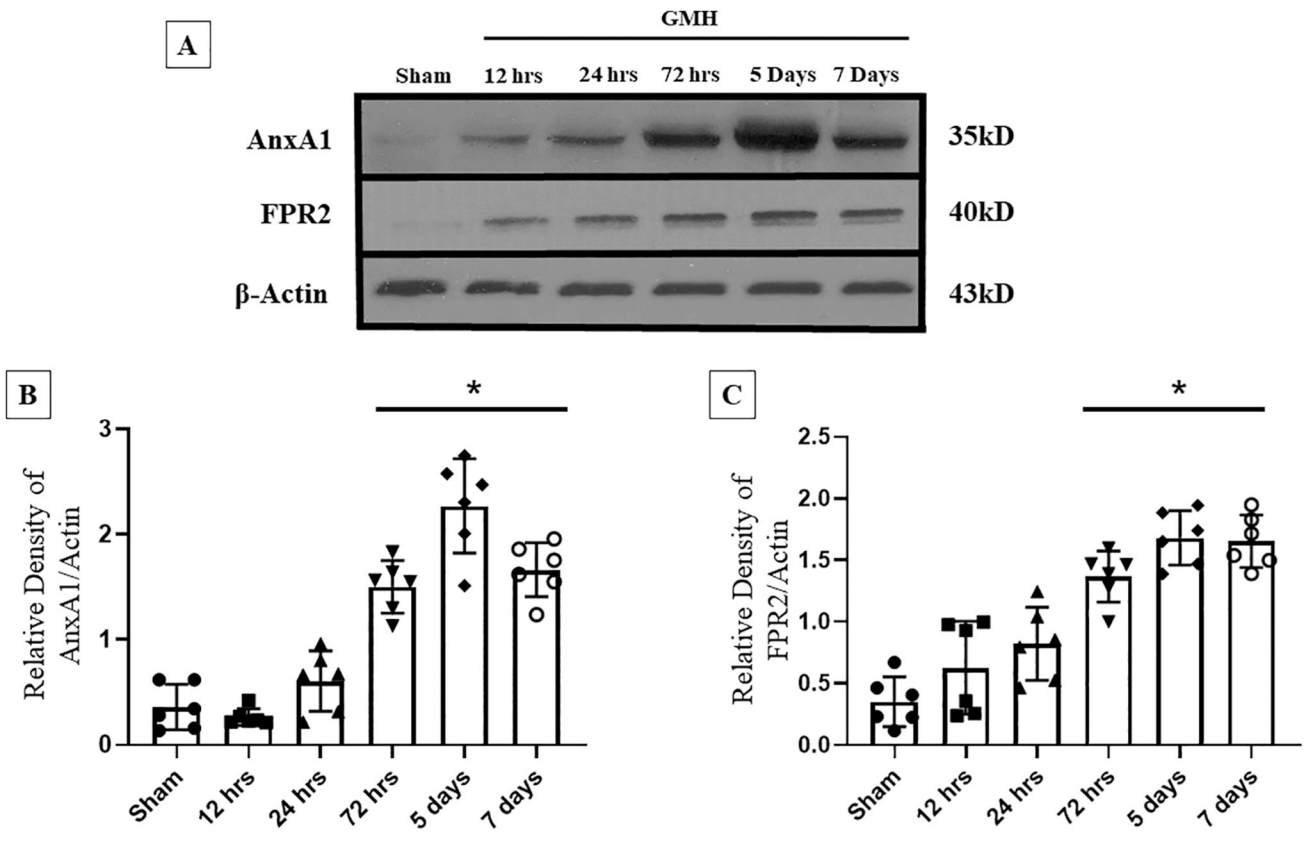

Fig. 2.

The time-course of endogenous levels of Annexin A1 and FPR2 after Germinal Matrix Hemorrhage. Western Blot was performed to detect endogenous expression of AnxA1 and FPR2 at 0 h (sham), 12 h, 24 h, 72 h, 5 days, and 7 days. A) Representative Bands of AnxA1, FPR2, and β-Actin. B) The expression of AnxA1 throughout different time-points. C) The Expression of FPR2 at different time-points. $n = 6$. Mean ± SD; one-way ANOVA followed by Tukey's test. * $p < 0.05$ vs. sham.

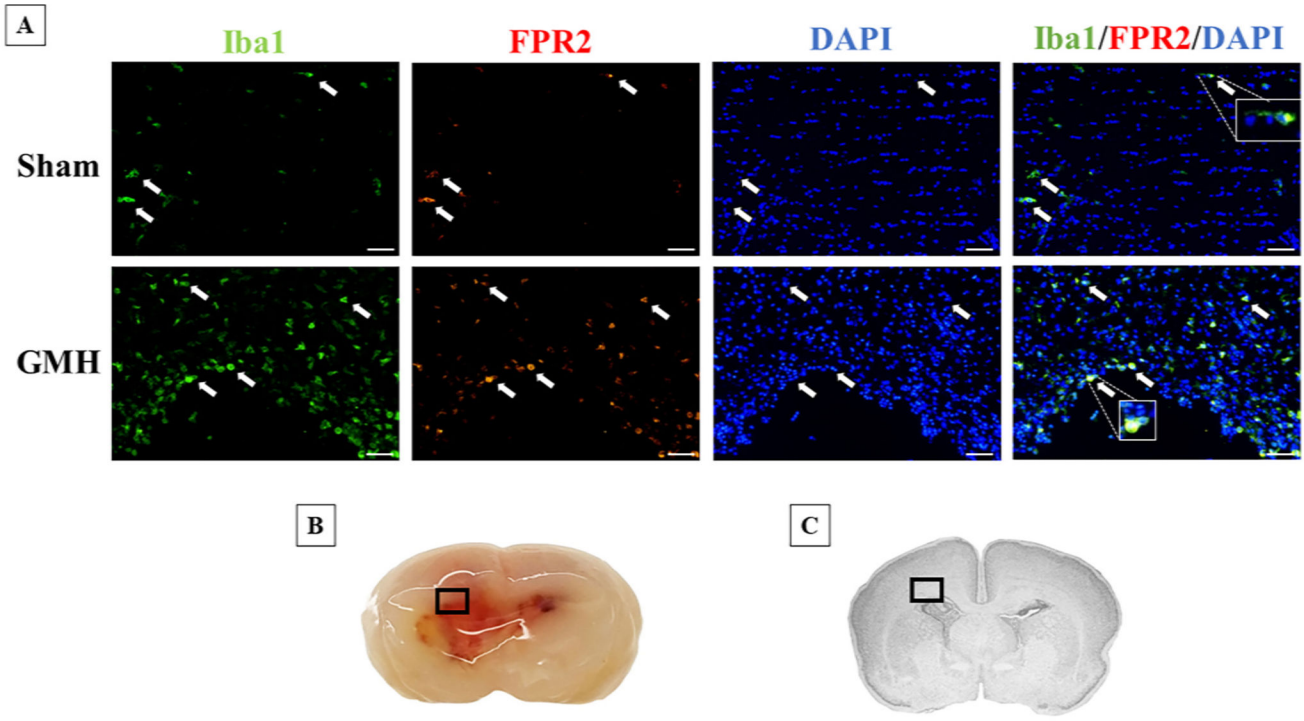

Fig. 3.

Colocalization of FPR2 and Iba1at 72 h after GMH. A) Immunohistochemistry was performed to detect FPR2 (red) and Iba1 (green) in Sham and Vehicle at 72 h after GMH induction. Positive FPR2 microglia cells are indicated by the arrows. Proteins are co-stained with DAPI (blue). B) A representative picture of the location of where the image was captured. C) Nissl-stained brain indicating the location of captured images. Scale bar = 20 μm.

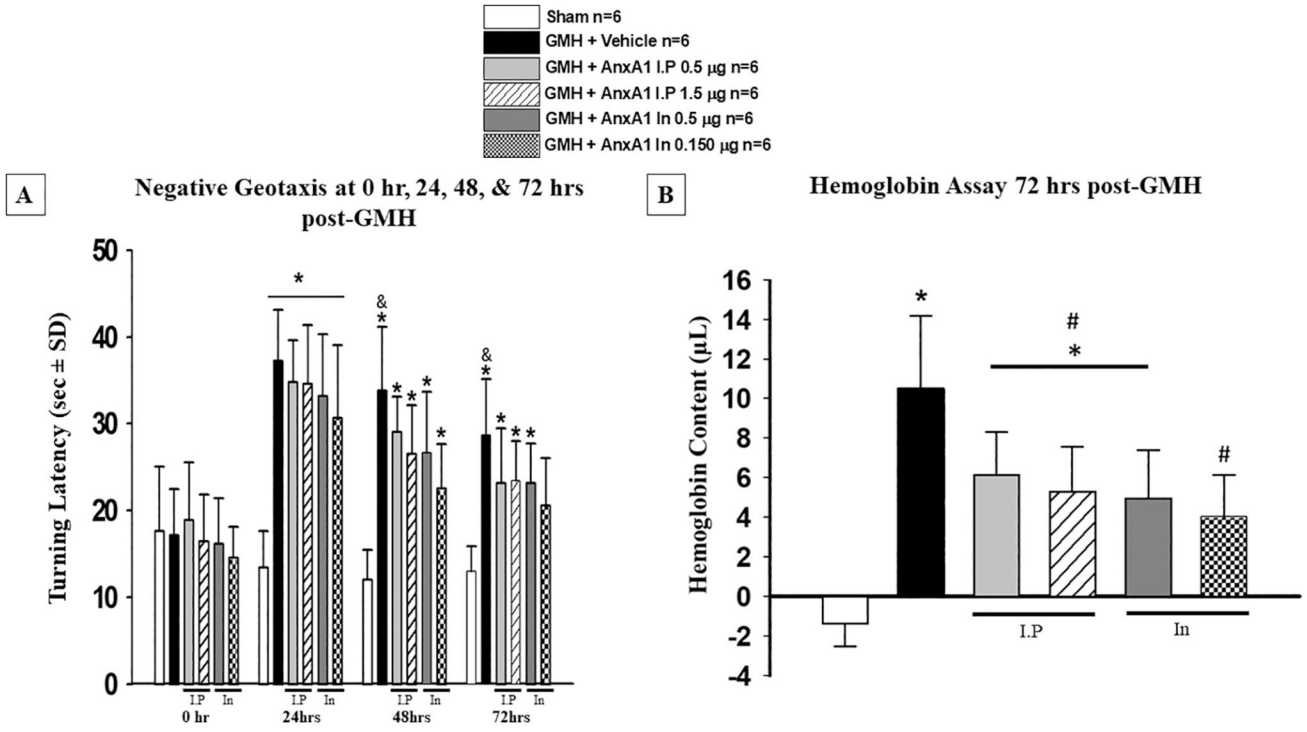

Fig. 4.

Dose Response study to determine the best effective dose and route of administration. A) Negative geotaxis was used to assess neurobehavioral function at 0, 24, 48, and 72 h. B) hemoglobin assay was conducted at 72 h post-GMH. All dosing regimens significantly reduced hemoglobin content at 72 h after GMH induction. $n = 6$. Mean ± SD; one-way ANOVA followed by Tukey's test. * $p < 0.05$ Vs. sham, # $p < 0.05$. Vs. Vehicle, & $p < 0.05$ Vs. AnxA1 In 0.150 µg. Bar under figures indicates which animals received intraperitoneal (I·P) or Intranasal (In) administration of AnxA1.

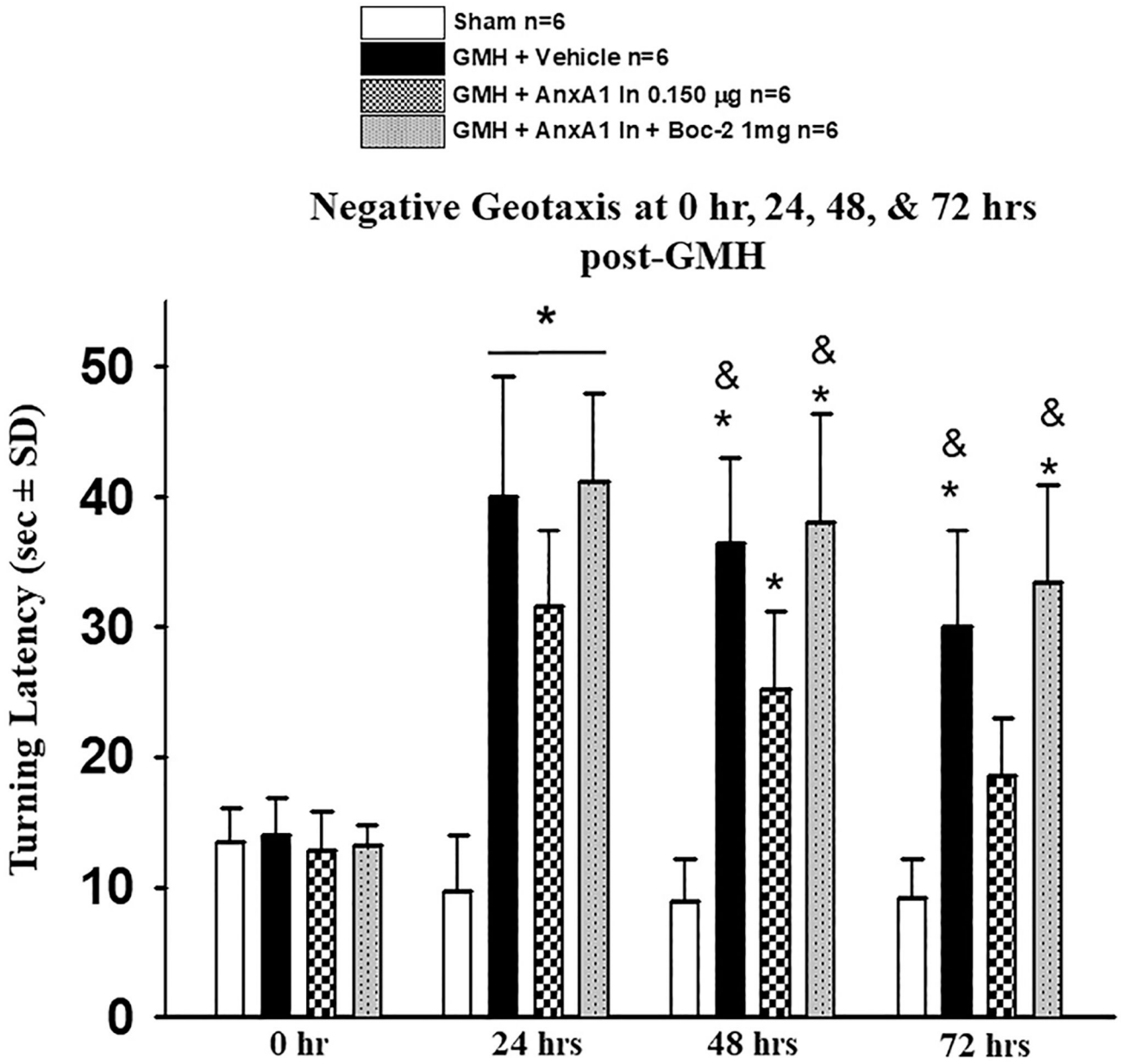

Fig. 5.

Pharmacological inhibition of FPR2 attenuated the protective effects of AnxA1 treatment at 2 and 3 days after GMH Induction. AnXA1 treated groups showed significant improvements in neurobehavior at 2 and 3 days. FPR2 inhibitor Boc-2 reversed the protective effects of Annexin A1 at 2 and 3 days after GMH. n = 6. Mean ± SD; one-way ANOVA followed by Tukey's test. * $p < 0.05$ vs. Sham, & $p < 0.05$ vs. AnxA1.

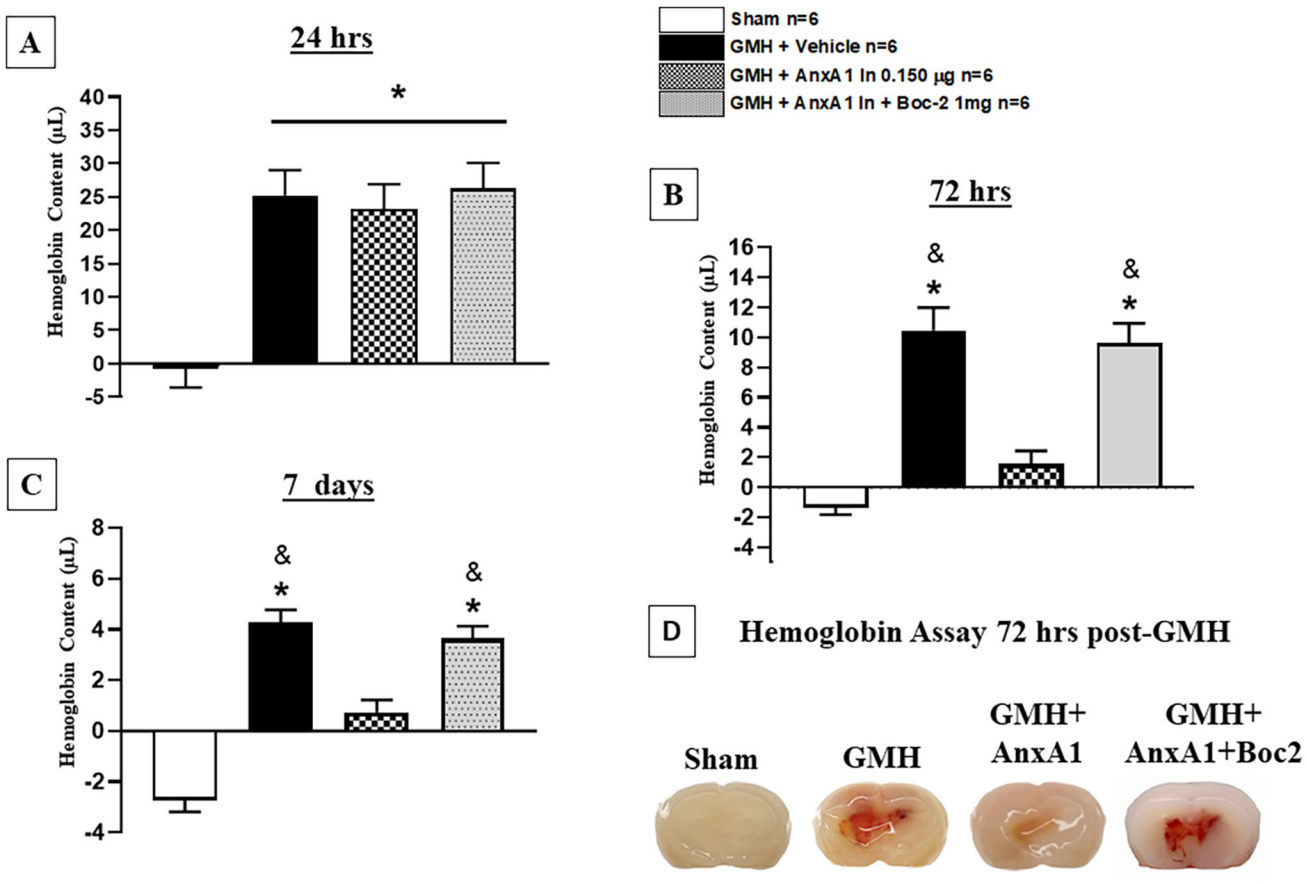

Fig. 6.

Annexin A1 treatment decreased hematoma volume at 72 h and 7 days after germinal matrix hemorrhage. Hemoglobin Assay was performed at A) 24 h, B) 72 Hrs, and C) 7 days after GMH. D) representative picture of the progression of hematoma resolution at 72 h. AnXA1 significantly reduced hematoma volume at 72 h (B and D) and 7 days (C) after GMH, yet boc-2 reversed these effects. $n = 6$. Mean ± SD; one-way ANOVA followed by Tukey's test. * $p < 0.05$ vs. sham. & $p < 0.05$ vs. AnxA1.

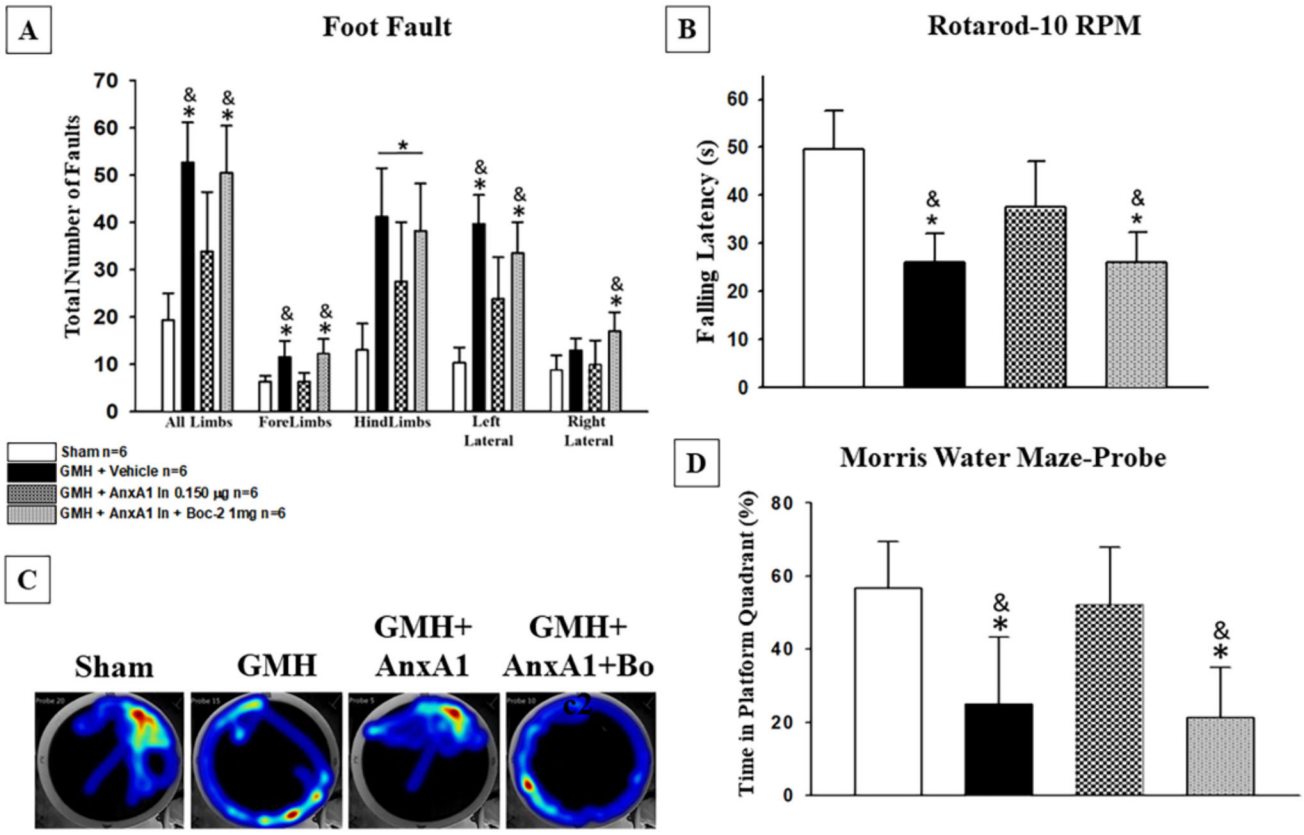

Fig. 7.

Annexin A1 improved locomotor, motor coordination, and memory at 4 weeks post-GMH, Boc-2 attenuated these effects. A) Annexin A1 Treatment improved locomotor coordination 4 weeks post-ictus, C) treated animals significantly improved motor coordination, and C —$D_)$ treated animal groups significantly improved in reference memory. FPR2 inhibitor reversed these effects. $n = 6$. Mean ± SD; one-way ANOVA followed by Tukey's test. * $p < 0.05$ vs. sham. & $p < 0.05$ vs. AnxA1.

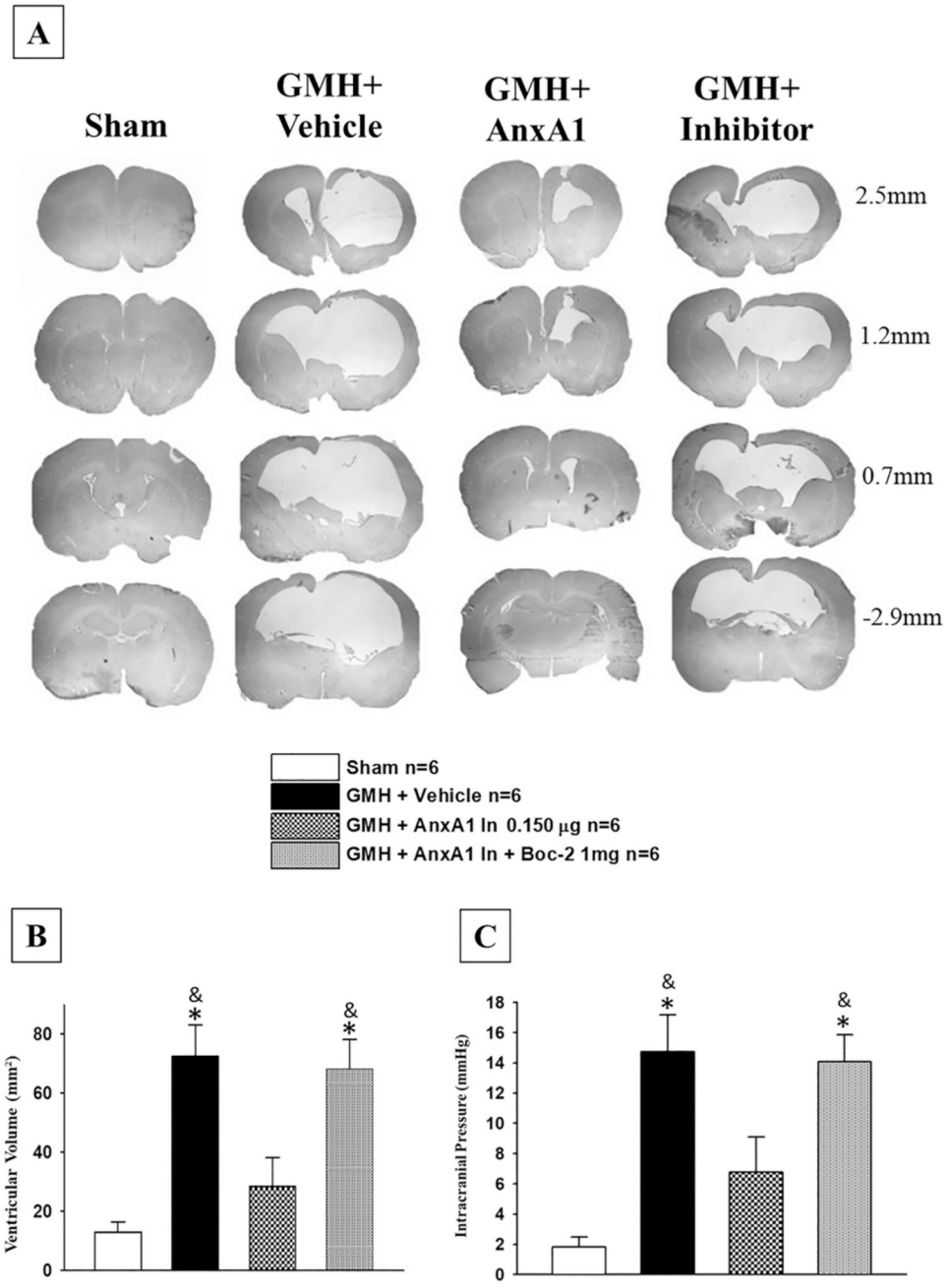

Fig. 8.

Annexin A1 treatment reduced ventricular dilation and intracranial pressure at 4 weeks after GMH. A and B) AnXA1 treated groups decreased ventricular dilation. Yet, FPR2 inhibitor Boc-2 reversed these effects. C) Annexin A1 significantly reduced CSF pressure when compared to both vehicle groups and Boc-2 + AnxA1 group. $n = 8$. Mean ± SD; one-way ANOVA followed by Tukey's test. * $p < 0.05$ vs. sham. & $p < 0.05$ vs. AnxA1. mmHG, millimeters of Mercury. Note: measurement on the right side of the representative pictures indicates the location of the brain section from bregma.

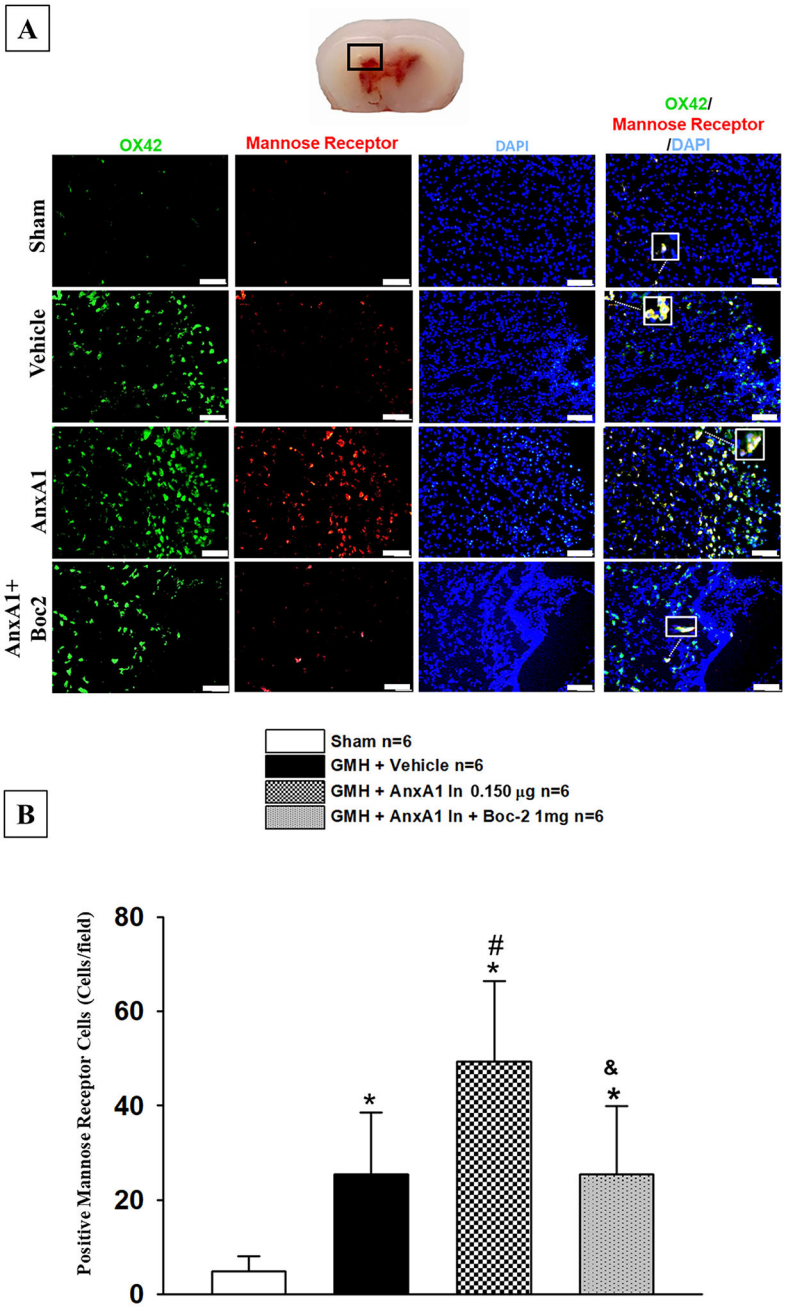

Fig. 9.

Annexin A1 treatment significantly increased M2 cells. Immunohistochemistry was performed to detect activated microglia (OX42;Green) and Mannose Receptor (Red) in all animal groups at 72 h after GMH induction. Annexin A1 increased M2 microglia cells at the site of perihematomal, and Boc-2 reversed these effects (Fig. 8A). Additionally, M1 microglia expression was reduced in the treated group (Fig. 8B). Scale bar = 20 µm. n = 6. Mean ± SD; one-way ANOVA followed by Tukey's test. * $p < 0.05$ vs. sham. & $p < 0.05$ vs. AnxA1.

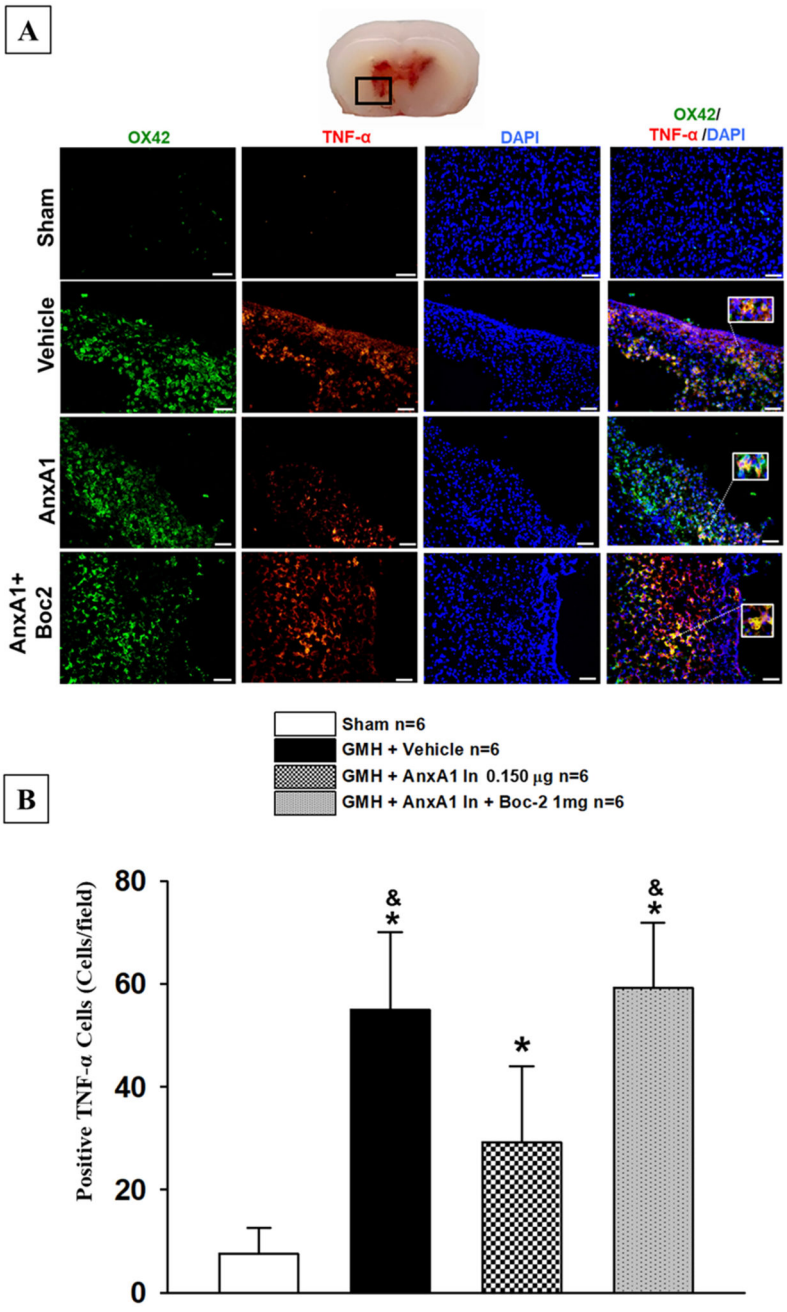

Fig. 10.

Annexin A1 treatment significantly decreased M1 cells after GMH. Immunohistochemistry was performed to detect activated microglia (OX42;Green) and M1 Marker (TNF-α;Red) in all animal groups at 72 h after GMH induction. Annexin A1 significantly decreased M1 microglia (TNF-α;Red) expression and Boc-2 reversed these effects (Fig. 8A). Scale bar = 20 µm. n = 6. Mean ± SD; one-way ANOVA followed by Tukey's test. * $p < 0.05$ vs. sham. & $p < 0.05$ vs. AnxA1.

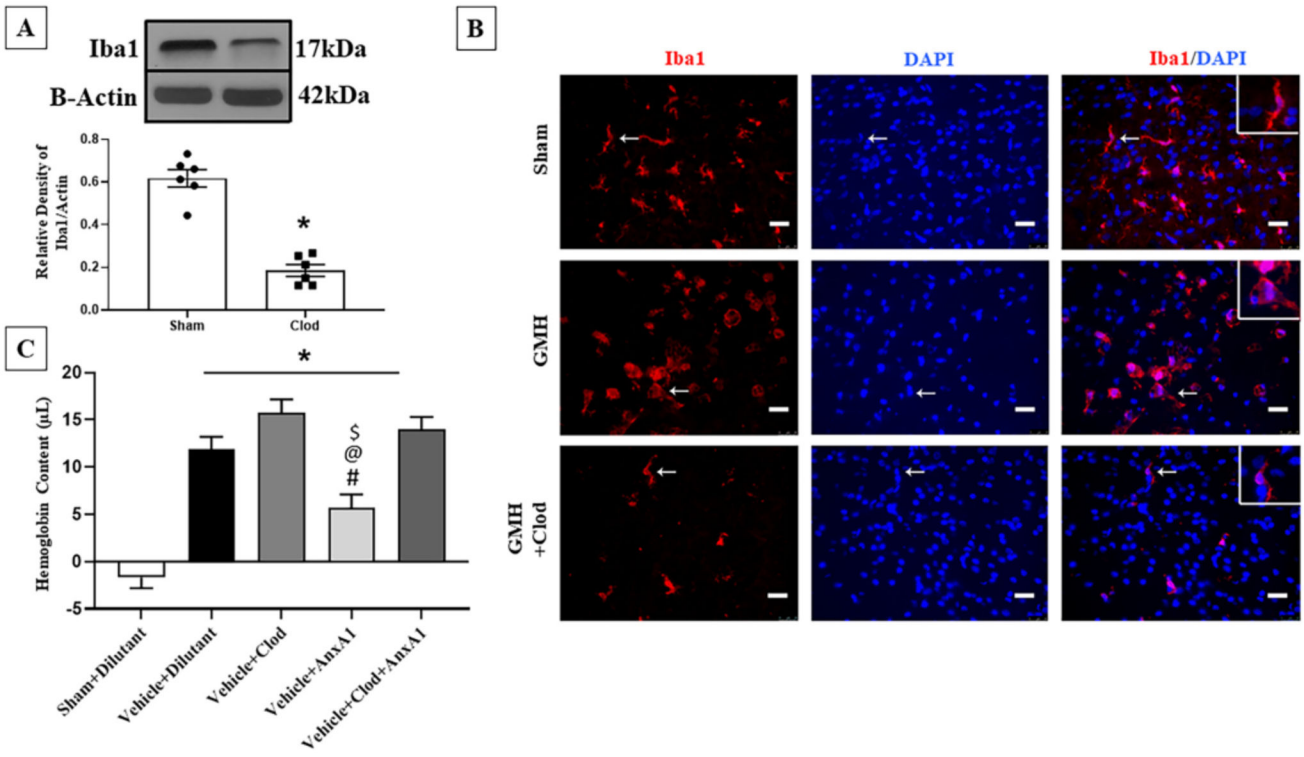

Fig. 11.

Inhibition of microglia cells ameliorates AnxA1 treatment effects on hematoma resolution. A) Western Blot at 24 h confirmed the inhibition of microglia in the neonatal CNS. B) IHC demonstrated the decreased presence of microglia cells (red) 24 h after GMH. C) Hemoglobin assay at 72 h demonstrated AnxA1 treatment had no effect on hematoma content. n = 6, Mean ± SD; *t*-test, one-way ANOVA followed by Tukey's test. * $p < 0.05$ vs. sham, # $p < 0.05$ vs. Vehicle, @ $p < 0.05$ vs. Vehicle+Clod, $ $p < 0.05$ Vehicle+Clod+AnxA1.

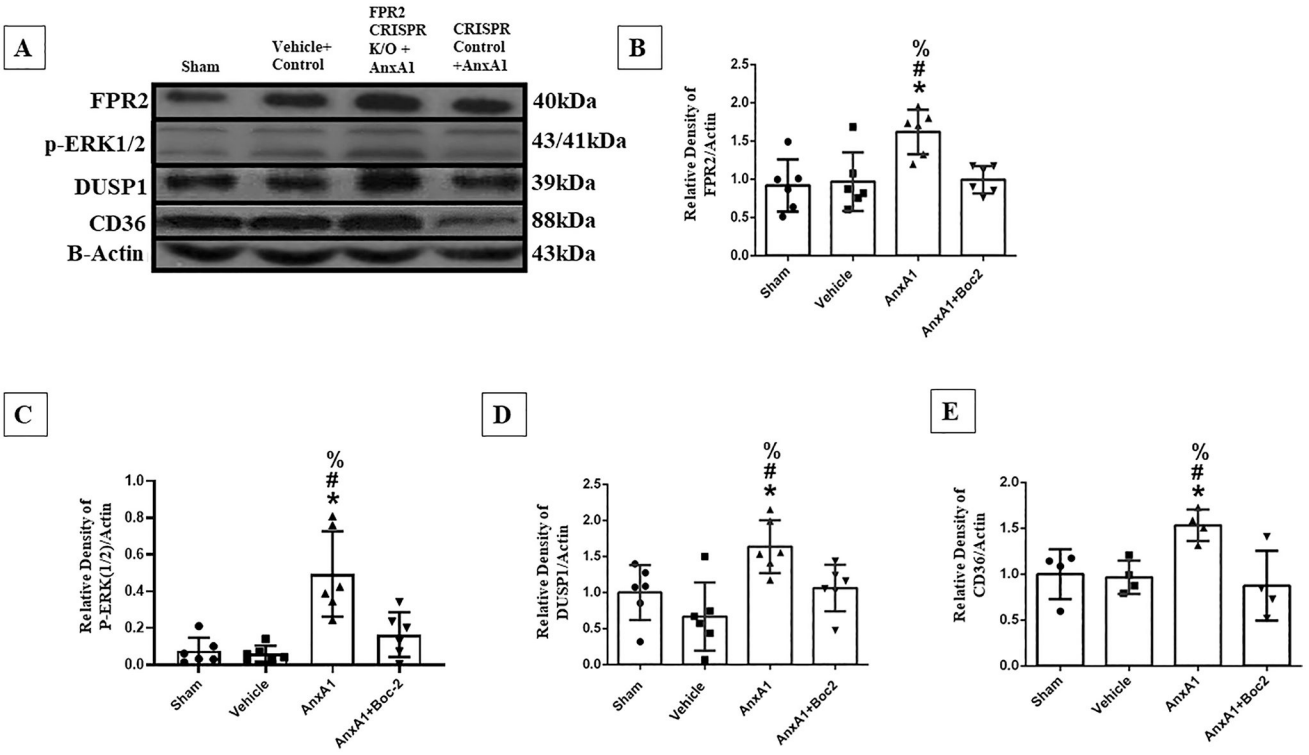

Fig. 12.

Annexin A1 treatment increased the expression of FPR2, p-ERK1/2, DUSP1, and CD36 72 h post-GMH. A) Protein expression of FPR2, p-ERK1/2, DUSP1, and CD36 were measured 72 h post-ictus. FPR2 (B), p-ERK1/2 (C), DUSP1 (DC), and CD36 (E) expression was shown to be signifcantly induced in the treated group compared to vehicle. n = 6. Mean ± SD; one-way ANOVA followed by Tukey's test. * $P < 0.05$ vs. sham, # $P < 0.05$ vs. Vehicle, & $P < 0.05$ vs. AnxA1, % $P < 0.05$ AnxA1 + Boc-2.

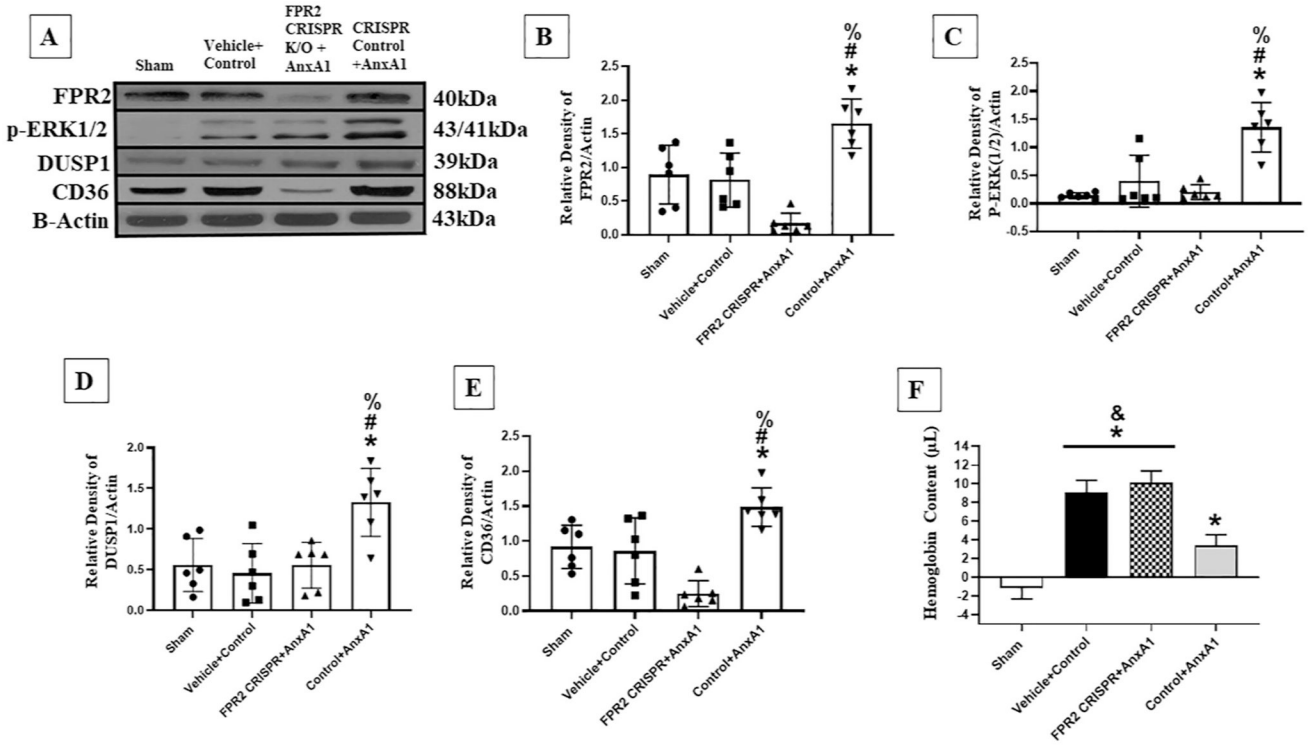

Fig. 13.

FPR2 CRISPR inhibited the upregulation of FPR2, p-ERK1/2, DUSP1, and CD36 after AnxA1 treatment at 72 h post-GMH. A) Protein expression of FPR2, p-ERK1/2, DUSP1, and CD36 were measured 72 h post-ictus. FPR2 (B), p-ERK1/2 (C), DUSP1 (D), and CD36 (E) expression was shown to be signifcantly decreased in the FPR2 CRISPR with treatment when compared to the AnxA1 control group. Hemoglobin assay was done at 72 h after GMH. FPR2 CRISPR inhibited the AnxA1 hematoma resolving effects when compared to the control treatment group (E). n = 6. Mean ± SD; one-way ANOVA followed by Tukey's test. * $P < 0.05$ vs. sham, # $P < 0.05$ vs. Vehicle, & $P < 0.05$ vs. AnxA1, % $P < 0.05$ AnxA1 + Boc-2.